

Potential Use of Sub-250 Gram Class UAVs for Rapid and Cost-Effective Aerial Mapping: A Case Study at Walimpong Dam, Indonesia

Mohammad Fuady Rusnadi ^{1,2}, I Gde Budi Indrawan ^{1*}, and Ferian Anggara ¹

¹ Geological Engineering Department, Faculty of Engineering, Gadjah Mada University, Yogyakarta, Indonesia

² Ministry of Public Works, Jakarta, Indonesia

[*igbindrawan@ugm.ac.id](mailto:igbindrawan@ugm.ac.id)

Abstract Topographic mapping plays a crucial role in a wide range of applications, from regional development to disaster mitigation. Aerial mapping using unmanned aerial vehicles (UAVs) has become increasingly popular due to its efficiency in covering large areas within a short time frame. However, conventional UAV-based mapping often involves high operational costs and is subject to stringent regulatory requirements, necessitating certified personnel for its operation. Recent advancements have introduced affordable sub-250 gram UAVs, which fall into a weight class with fewer regulatory constraints, that are capable of performing automated aerial mapping. This situation presents an opportunity to enhance the accessibility of aerial mapping technologies, particularly for non-specialist users. This study investigates the potential of sub-250 gram UAVs for aerial mapping by conducting a case study at the proposed site of the Walimpong Dam in Soppeng Regency, South Sulawesi Province, Indonesia. The UAV was flown autonomously in a grid pattern at a predetermined altitude. This paper will also present a comparison of the capabilities between sub-250 gram UAV and UAVs weighing more than 250 grams. The comparative analysis demonstrates that the mapping capability achieved by the sub-250 gram UAV closely approximates that of its heavier counterpart. These findings suggest that lightweight UAVs can serve as a viable alternative for aerial mapping tasks, potentially broadening participation and fostering inclusivity in geospatial data acquisition and mapping sciences.

Keywords: Aerial Mapping, Remote Sensing, Unmanned Aerial Vehicle, Walimpong Dam

1. Introduction

Topographic mapping plays a crucial role in a wide range of applications, from providing essential information on terrain and elevation for infrastructure development such as roads, bridges, and dams, to supporting the identification of flood-prone and landslide-susceptible areas in the context of disaster mitigation (Herrera, 2024). Various methods are available for producing topographic maps, including ground surveying, satellite based remote sensing, and aerial mapping through photogrammetry or LiDAR techniques. Due to its ability to acquire spatial data in a cost-effective and rapid manner, photogrammetric mapping using unmanned aerial vehicles (UAVs) has become a popular option for generating topographic

maps (Pathak et al., 2024).

While UAV-based aerial mapping has become relatively more affordable in recent years, its accessibility is still largely limited to practitioners and professionals. This limitation arises because until recently, UAVs capable of executing autonomous mapping missions were available only in certain series—for example, the DJI Mavic 3 Enterprise, which at the time of writing, is marketed starting from USD 4,175 (DJI Retail, 2025). Beyond the relatively high price point for casual users, UAVs equipped with autonomous mapping capability generally weigh more than 250 grams. Under aviation regulations in several countries, including those of the Federal Aviation Administration (United States) and the Civil Aviation Authority (United Kingdom), operating UAVs exceeding 250 grams requires the pilot to obtain an Operator ID and register the aircraft with the relevant authority. Consequently, such regulatory requirements further constrain the accessibility of aerial mapping for novice or non-professional users.

Sub-250 gram UAVs, which have been classified into the toy category and lacked autonomous mapping capabilities, have recently been enabled by manufacturers to perform autonomous aerial mapping missions. This advancement has been made possible through the release of software development kits (SDKs) in recent years, which provide tools that allow third-party developers to create applications enabling sub-250 gram UAVs to carry out autonomous mapping tasks. One such example of an affordable sub-250 gram UAV that previously could not perform autonomous aerial mapping missions is DJI Mini 3. However, in 2023 the manufacturer began providing SDK access, and by 2024 third-party applications for autonomous aerial mapping compatible with the DJI Mini 3 had become available.

To evaluate the capabilities of sub-250 gram UAVs in conducting aerial mapping, a topographic mapping trial will be carried out using a sub-250 gram UAV at the proposed site of the Walimpong Dam. The dam is planned to be constructed by the Ministry of Public Works in Marioriwawo District, Soppeng Regency, South Sulawesi, and the location map is presented in Figure 1. This site was selected for the trial because comprehensive topographic mapping is essential in dam construction, as reservoir characteristics are closely related to elevation and surface area (Chow et al., 1988). In addition to the aerial mapping trial, a comparative assessment will also be conducted between sub-250 gram UAVs and professional UAVs weighing over 250 grams, focusing on parameters that influence the quality of mapping outcomes.

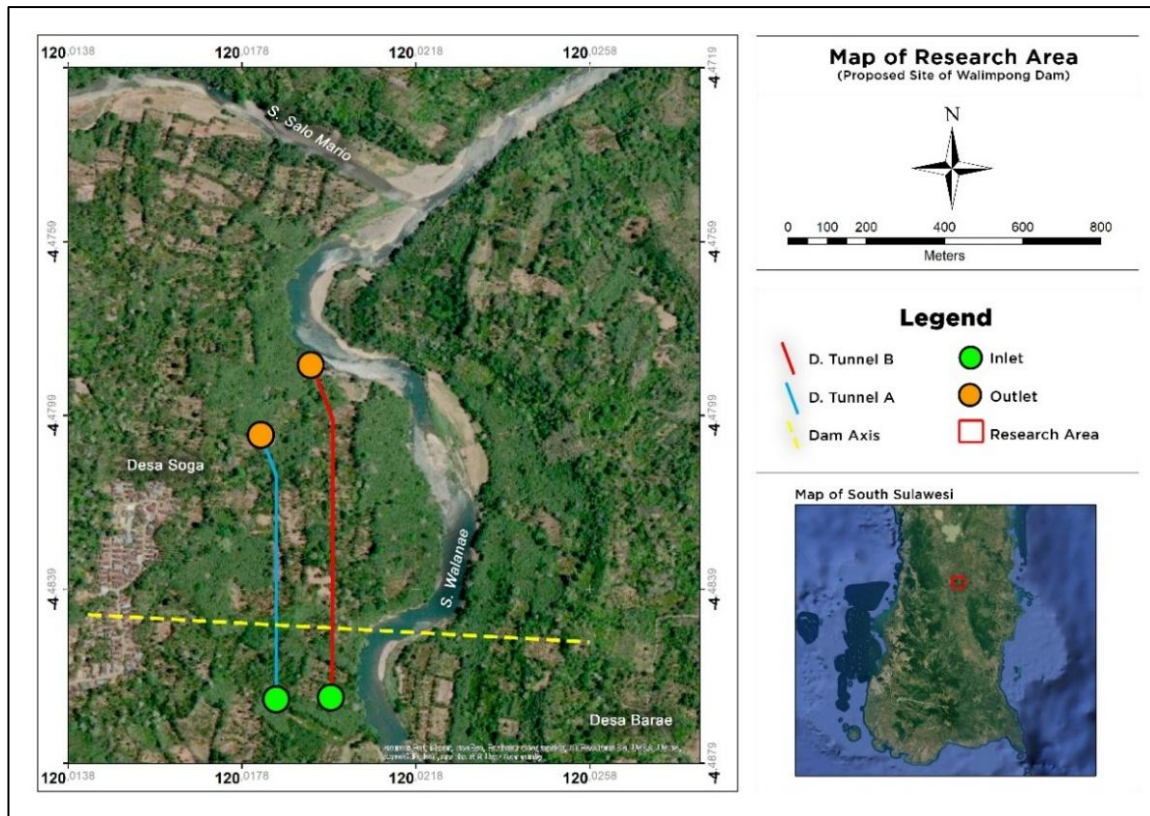


Figure 1. Map of Proposed Site of Walimpong Dam
(Modified from Google Earth Imagery, retrieved in 2025)

By assessing the aerial mapping capabilities of sub-250 gram UAVs and comparing them with professional UAVs that are already widely used, this study aims to broaden accessibility for non-expert users with limited resources to engage in mapping and remote sensing. Greater participation from the wider community in these fields is expected to contribute to the advancement of knowledge and foster new discoveries in the future.

2. Tools and Methodology

2.1. Unmanned Aerial Vehicle (UAV)

A UAV is commonly defined as a pilotless aircraft capable of flying and remaining airborne without the need for an onboard human operator, offering more cost-efficient operations compared to equivalent manned systems (Mohsan et al., 2022). In this study, three types of UAVs were used to represent each distinct category (Figure 2), with their key specifications presented in Table 1.



Figure 2. UAV used in this study;
(a) DJI Phantom 4 Pro, (b) DJI Matrice 300 RTK, (c) DJI Mini 3

Table 1. UAV model and key specification (Source: DJI)

Model	DJI Mini 3	DJI Phantom 4 Pro	DJI Matrice 300 RTK + Zenmuse L1 Sensor
Release Year	2022	2016	2020
Category	Entry Level	Advanced	Professional
Weight	248 gram	1388 gram	6300 gram
Sensor Size	1/1.3 inch (9.8 mm × 7.35 mm)	1 inch (23.83 mm × 8.56 mm)	1 inch (12.83 mm × 8.56 mm)
Focal Length	6.72 mm	8.6 mm	8.8 mm
Resolution	12 megapixel (4000 × 3000 pixel)	20 megapixel (5472 × 3648 pixel)	20 megapixel (5472 × 3648 pixel)
Max Speed	58 km/h	72 km/h	83 m/s
Max Flight Time	38 minutes	30 minutes	55 minutes

2.2. Aerial Mapping

UAV-based aerial mapping was employed in this study to obtain topographic data rapidly and efficiently. The process began with flight path planning, including the adjustment of altitude and flight speed, camera parameters, and the degree of image overlap. Data acquisition was then carried out by flying the UAV over the mapping area. The collected images were subsequently processed using photogrammetric software based on the Structure from Motion (SfM) approach, producing a dense point cloud, orthomosaic imagery, and a digital elevation model of the mapped area (Nex & Remondino, 2013). In this study, trials conducted with a

sub-250 gram UAV were evaluated in terms of mapping efficiency, coverage area, and the level of detail in the mapping results.

2.3. Ground Sampling Distance

Ground Sampling Distance (GSD) is one of the key parameters in UAV-based aerial photogrammetry. GSD is defined as the ground surface area represented by a single pixel in a digital image. In other words, the smaller the GSD value, the higher the level of spatial detail that can be obtained from the mapping results (Eisenbeis, 2009). Mathematically, GSD can be calculated using the following equation (Fakhri et al., 2023):

(1)

$$GSD = \frac{Sw \times H}{Fl \times imW}$$

Where:

- Sw = sensor width
- H = flight altitude
- Fl = focal length
- imW = image width

From the equation above, it can be concluded that the specifications of the sensor and lens, along with the flight altitude (i.e., the distance between the sensor and the measured surface), have a major influence on the resulting GSD value.

2.4. Individual Image Quality Test

The quality of individual images captured by UAV cameras plays a crucial role in determining the accuracy of photogrammetric mapping. Structure-from-Motion (SfM) reconstruction heavily relies on the ability to detect and match tie points across images. High-quality photographs with sharpness, adequate contrast, and minimal distortion enable accurate identification of tie points, thereby facilitating the construction of reliable 3D models. Conversely, low-quality images—such as those affected by blur, overexposure or underexposure, or excessive noise—reduce the number of detectable tie points and ultimately degrade the quality of the final products (Westoby et al., 2012).

Overall, the quality of individual images is highly influential in determining the spatial and geometric accuracy of photogrammetric mapping. Minor errors in the input imagery may accumulate, resulting in deformations in the orthomosaic and inaccuracies in the contour lines. Therefore, image quality control during the acquisition stage—including camera selection, exposure settings, and flight conditions—constitutes an essential component of UAV-based mapping methodologies.

The experiment will be conducted by capturing images of an object at a constant altitude, after which the photographic results from the three different UAVs will be compared. The evaluation focuses on image sharpness at the center and edges of the frame, as image sharpness is typically non-uniform across the entire frame, with the edges generally being the least sharp areas in a photograph (O'Connor, 2018).

3. Results and Discussion

3.1. Aerial Mapping

The planning and execution of aerial mapping with a sub-250 gram UAV at the proposed Walimpong Dam site were conducted using the Dronelink application. From the total mapping area of interest of 2 km², the flight mission was divided into four quadrants, each measuring 0.5 km², as illustrated in the flight plan shown in Figure 3. This division was necessary due to considerations of signal range and battery capacity.



Figure 3. Aerial mapping's flight plan of the proposed site of Walimpong Dam
(Modified from Dronelink, retrieved in 2025)

In the flight mission planning, several key flight parameters were configured, including flight altitude, flight speed, percentage of image overlap, and UAV gimbal pitch angle. The flight altitude was set at 119 meters above the take-off point. This altitude was selected because a higher altitude allows for greater mapping coverage (Seifert et al., 2019), while still remains below the maximum permitted altitude of 120 meters as regulated by the Indonesian Ministry

of Transportation (2020). The flight speed chosen for this mission was 30 km/h. Flight speed must be carefully considered, as higher speeds increase the likelihood of motion blur (Maes, 2025). The image overlap value was set to 90%, which is necessary since in areas with dense vegetation cover, the recommended overlap ranges from 80% to 90% (Frey et al., 2018). As gimbal pitch angle significantly affects aerial mapping coverage (Papaioannou et al., 2023), in addition to nadir photography, oblique imagery was also captured by adjusting the gimbal to a pitch angle of -40° to enhance mapping coverage.

From a total of eight flights (one nadir and one oblique flight in each quadrant), with a cumulative flight duration of 114 minutes or approximately 14 to 15 minutes per flight, 2,274 aerial images were collected. These images were subsequently processed using Pix4Dmapper software. The total processing time, from initial processing through the generation of the digital surface model (DSM) and orthomosaic, amounted to 13 hours and 25 minutes, although this duration is highly dependent on the processing power of the hardware used (Adrov et al., 2012). The overall mapping process produced a DSM and orthomosaic covering an area of 6.8 km², with an average ground sampling distance of 15.6 cm/pixel. However, it should be noted that not all parts of the 6.8 km² mapped area exhibited uniform data quality. At the edges of the mapping area, distortions were observed due to insufficient overlap, which reduced the number of tie points near the edges of the mapping area (Maes, 2025). The resulting DSM and orthomosaic are presented in Figure 4.

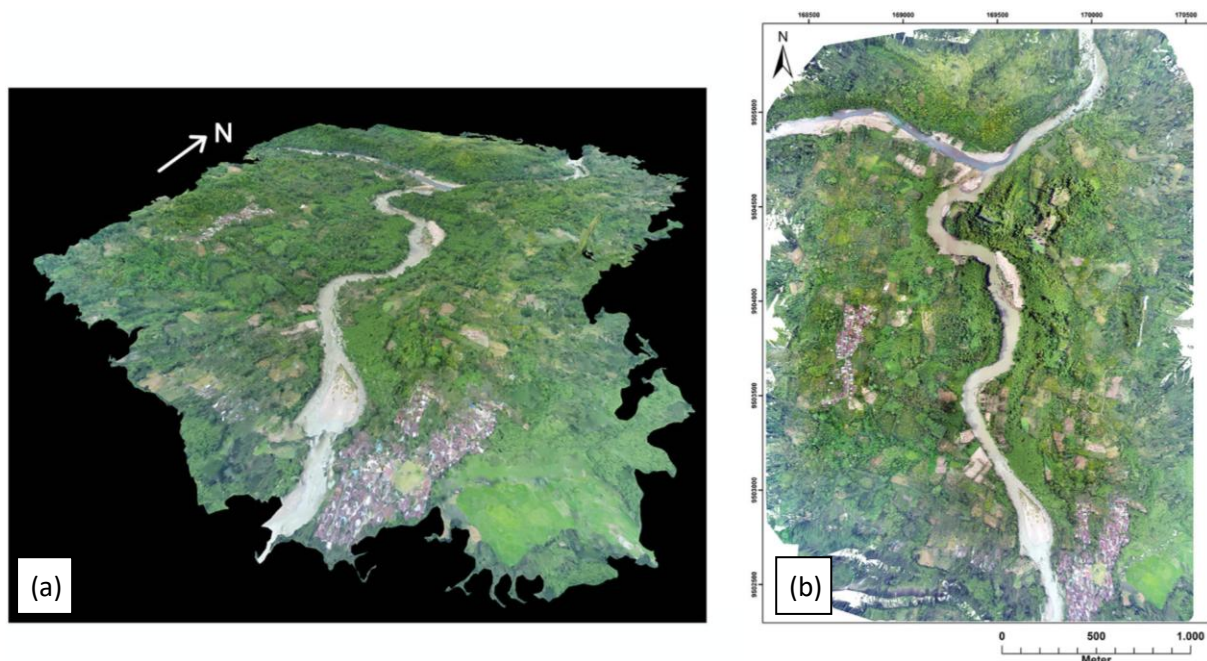


Figure 4. Mapping Results
(a) Digital Surface Model; (b) Orthomosaic

3.2. Ground Sampling Distance Comparison

The Ground Sampling Distance (GSD) value is one of the key parameters for evaluating the quality of photogrammetric data produced by a UAV, as it directly represents the ground object size corresponding to a single image pixel. Variations in camera specifications (sensor size, resolution, focal length) and flight altitude cause each UAV to produce different GSD values, even when operated over the same area and mission. UAVs equipped with high-resolution sensors and longer focal lengths generally yield smaller GSD values, thereby capturing surface details with greater spatial clarity. Conversely, UAVs with smaller sensors and limited resolution produce larger GSD values, resulting in the loss of fine details in both orthomosaics and digital elevation models. To assess the extent to which sub-250 gram UAVs can approach the performance of UAVs that are more commonly used for mapping, a comparison of the theoretical GSD values generated by each UAV at a flight altitude of 120 meters was carried out using Equation 1.

Table 2. GSD Comparison Between UAVs

UAV Model	Weight (gram)	Sensor Width (mm)	Image Width (pixel)	Focal Length (mm)	Flight Altitude (m)	GSD (cm/pixel)
DJI Mini 3	249	9.8	4,000	6.7	120	4.4
DJI Phantom 4 Pro	1,388	12.833	5,472	8.6		3.3
DJI Matrice 300 + Zenmuse L1	6,300	12.833	5,472	8.8		3.2

From the comparison above, it can be seen that theoretically, the sub-250 gram UAV had a GSD difference of approximately 1.2 cm/pixel, or about 37.5% lower than the heavier and more advanced UAVs. This difference is primarily due to the variation in sensor size between the UAVs being compared.

3.3. Individual Image Comparison

The quality of individual images produced by each UAV plays a critical role in determining the overall quality of photogrammetric mapping, as the Structure-from-Motion (SfM) process strongly depends on image sharpness and feature readability, which control the number of detectable tie points. In this subsection, a comparison is presented of image quality from three types of UAVs captured at an altitude of ten meters using a test chart. The evaluation focuses on image quality and distortion at both the center and edges of the frame, since image sharpness

is generally non-uniform across the frame, with the edges typically being the least sharp areas of a photograph. The comparison of the full images, center-frame crops, and edge-frame crops from the three UAVs is shown in the figure below.

From the comparison of images captured by the three UAVs, it is evident that the line sharpness on the test chart—both at the center and at the edges of the frame—is just slightly higher in the photographs produced by the DJI Phantom 4 Pro and DJI Matrice 300 than in those from the DJI Mini 3. Regarding distortion, the DJI Mini 3 displayed purple fringing due to chromatic aberration near the frame edges, while the DJI Matrice 300 exhibited a noticeable barrel distortion across the image, which could potentially degrade reconstruction quality if left uncorrected (Remondino & Fraser, 2006; Terpstra et al., 2017).

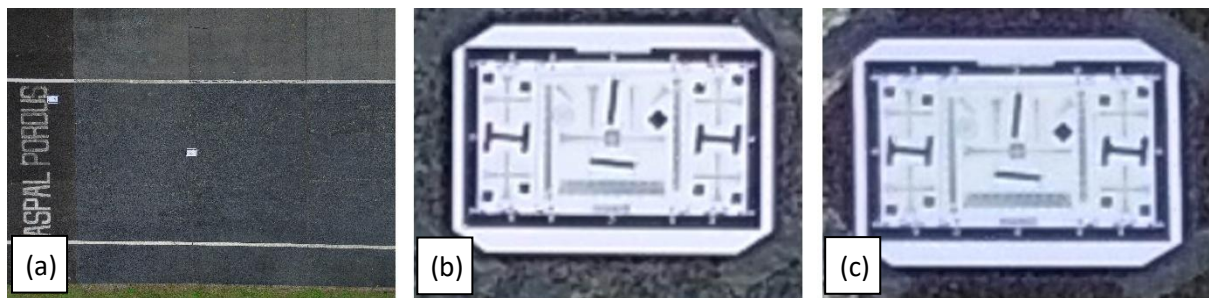


Figure 5. Individual image from DJI Mini 3
(a) Full; (b) Center Crop; (c) Edge Crop

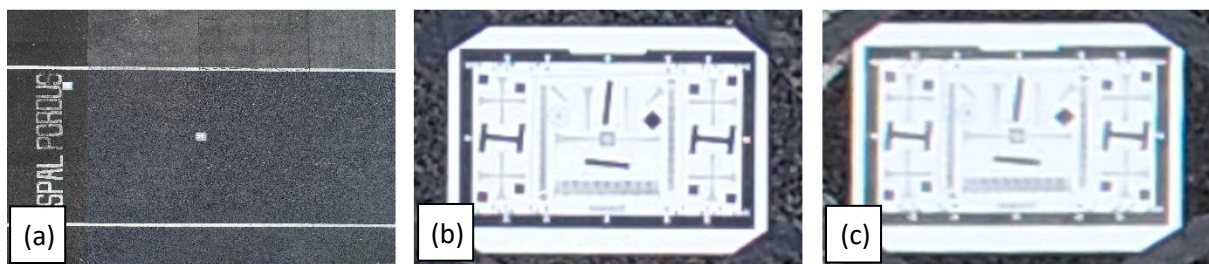


Figure 6. Individual image from DJI Phantom 4 Pro
(a) Full; (b) Center Crop; (c) Edge Crop

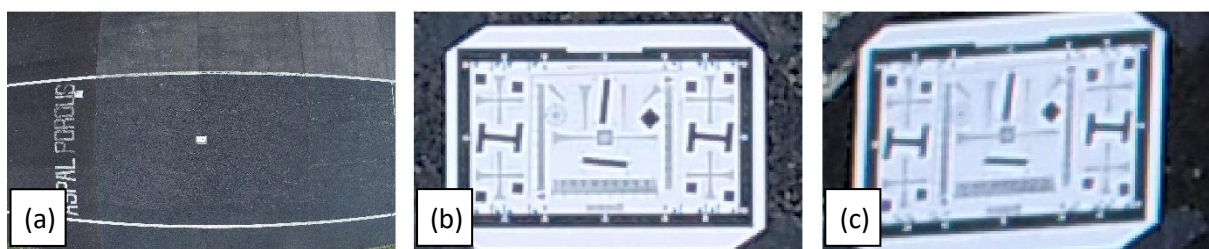


Figure 7. Individual image from DJI Matrice 300 + Zenmuse L1
(a) Full; (b) Center Crop; (c) Edge Crop

3.4. Comparison of Flight Performance, Safety, and Additional Features

Although the tests presented in Section 3.1 demonstrated that sub-250 gram UAVs are capable of conducting aerial mapping missions with reasonable coverage and resolution, several limitations need to be considered. First, in order to maintain the UAV's weight below 250 grams, manufacturers have compromised on battery capacity, which directly affects flight duration. Second, there are constraints related to autonomous mission execution. Since the onboard computer is not designed to store flight plans internally, flight commands must be continuously transmitted from the controller throughout the mission. As a result, the mission may be interrupted or even fail if communication between the UAV and the controller is disrupted. This situation contrasts with professional UAVs, which are typically equipped with onboard mission storage, allowing them to continue along the preprogrammed flight path even if communication with the controller is lost.

Third, regarding safety features, the tested sub-250 gram UAV lacked an obstacle avoidance system, a feature commonly integrated into professional UAVs. This absence increases the risk of collisions, particularly when operating in environments with numerous obstacles such as trees, buildings, or power lines. Consequently, mapping with UAVs that do not have obstacle avoidance must be carried out strictly within visual line of sight.

Fourth, in terms of navigation capability, sub-250 gram UAVs are generally equipped only with standard navigation systems. By contrast, professional UAVs often include advanced navigation technologies, with some models already supporting real-time kinematic (RTK) corrections, thereby providing much higher positional accuracy.

Fifth, there is a limitation in payload flexibility. Sub-250 gram UAVs cannot accommodate a wide range of sensors as professional UAVs can, such as LiDAR or multispectral cameras, which significantly broaden the scope of possible missions.

Finally, sub-250 gram UAVs currently lack official software support from manufacturers for both flight mission planning and data reconstruction, in contrast to the integrated solutions typically provided for professional UAVs.

4. Conclusion and Recommendation

The findings from the study conducted at the proposed site of Walimpong Dam demonstrate that sub-250 gram UAVs possess significant potential for aerial mapping applications. Although variations in Ground Sampling Distance (GSD) and individual image quality were

observed when compared with professional UAVs, the generated orthomosaic and digital surface model were able to represent topographic conditions reliably for detailed-scale mapping. Consequently, sub-250 gram UAVs may serve as a cost-effective alternative for geospatial data acquisition, particularly for non-specialist users or organizations with limited resources.

Nevertheless, the limitations of sub-250 gram UAVs cannot be overlooked. The small battery capacity restricts flight duration, while the absence of RTK support may reduce positional accuracy. From an operational perspective, the lack of an obstacle avoidance system, payload restrictions to only the built-in camera, and the inability to store missions onboard increase risks and reduce flight reliability. Furthermore, the limited availability of official software support further constrains the functionality of this UAV class compared with professional models.

Based on these findings, sub-250 gram UAVs are recommended for small- to medium-scale mapping missions, particularly for research, education, and preliminary surveys where low cost and high accessibility are essential. For large-scale missions, complex terrain conditions, or applications demanding high positional accuracy, professional UAVs remain the preferred option. With the continued advancement of software and hardware support for sub-250 gram UAVs, it is expected that these limitations will gradually diminish, enabling aerial mapping technologies to become more inclusive and accessible across diverse user groups.

5. Acknowledgements

The author would like to express sincere gratitude to the Ministry of Public Works for granting the opportunity to pursue further education through the 2024 Super Specialist Scholarship Program; to the Pompegan Jeneberang River Basin Authority for providing access to conduct research at the proposed site of Walimpong Dam; and to the Implementation Unit for Bridge and Tunnel Safety for kindly allowing the use of the equipments essential to the completion of this paper.

References

Adrov, V. N., Drakin, M. A., & Sechin, A. Y. (2012). High Performance Photogrammetric Processing on Computer Clusters. *The International Archives of the Photogrammetry, Remote Sensing and Spatial Information Sciences/International Archives of the*

- Photogrammetry, Remote Sensing and Spatial Information Sciences, XXXIX-B4*, 109–112. <https://doi.org/10.5194/isprsarchives-xxxix-b4-109-2012>
- Chow, V. T., Maidment, D. R., & Mays, L. W. (1988). *Applied Hydrology*. McGraw-Hill.
- DJI Retail. *DJI Mavic 3E Enterprise Basic Combo*. Retrieved August 2025, from <https://dji-retail.co.uk/products/dji-mavic-3-enterprise-drone>
- Fakhri, S. A., Motayyeb, S., Saadatseresht, M., Zakeri, H., & Mousavi, V. (2023). Comparison Of Uav Image Spatial Resolution Based On The Siemens Star Target. *ISPRS Annals of the Photogrammetry, Remote Sensing and Spatial Information Sciences, X-4/W1-2022*, 143–150. <https://doi.org/10.5194/isprs-annals-x-4-w1-2022-143-2023>
- Federal Aviation Authority. (2022). *How to Register Your Drone | FAA*. https://www.faa.gov/uas/getting_started/register_drone
- Frey, J., Kovach, K., Stemmler, S., & Koch, B. (2018). UAV Photogrammetry of Forests as a Vulnerable Process. A Sensitivity Analysis for a Structure from Motion RGB-Image Pipeline. *Remote Sensing, 10*(6), 912–912. <https://doi.org/10.3390/rs10060912>
- Henri Eisenbeiß. (2009). *UAV Photogrammetry*. Zurich: ETH Zurich.
- Herrera, G. (2024). Topographic Mapping in Environmental Impact Assessment. *Journal of Geography & Natural Disasters, 14*(1). <https://doi.org/10.35841/2167-0587.24.14.304>
- Kementerian Perhubungan Republik Indonesia. (2020). Peraturan Menteri Perhubungan Republik Indonesia Nomor PM 37 Tahun 2020 tentang Pengoperasian Pesawat Udara Tanpa Awak di Ruang Udara yang Dilayani Indonesia. <https://peraturan.bpk.go.id/Details/149457/permenhub-no-37-tahun-2020>
- Maes, W. H. (2025). Practical Guidelines for Performing UAV Mapping Flights with Snapshot Sensors. *Remote Sensing, 17*(4), 606. <https://doi.org/10.3390/rs17040606>
- Mohsan, S. A. H., Khan, M. A., Noor, F., Ullah, I., & Alsharif, M. H. (2022). Towards the Unmanned Aerial Vehicles (UAVs): A Comprehensive Review. *Drones, 6*(6), 147. <https://doi.org/10.3390/drones6060147>
- Nex, F., & Remondino, F. (2013). UAV for 3D mapping applications: a review. *Applied Geomatics, 6*(1), 1–15. <https://doi.org/10.1007/s12518-013-0120-x>
- O'Connor, J. (2018). *Impact of Image Quality on SfM Photogrammetry: Colour, Compression, and Noise*. Lancaster: Lancaster University.
- Papaoiannou, S., Kolios, P., Theocharides, T., Panayiotou, C. G., & Polycarpou, M. M. (2023). Integrated Guidance and Gimbal Control for Coverage Planning With Visibility Constraints. *IEEE Transactions on Aerospace and Electronic Systems, 1*–15. <https://doi.org/10.1109/taes.2022.3199196>
- Pathak, S., Acharya, S., Saugat Bk, Karn, G., & Thapa, U. (2024). UAV-based topographical mapping and accuracy assessment of orthophoto using GCP. *Mersin Photogrammetry Journal, 6*(1), 1–8. <https://doi.org/10.53093/mephoj.1350426>
- Remondino, F., & Fraser, C. (2005). Digital Camera Calibration Methods: Considerations and Comparisons. *The International Archives of the Photogrammetry, Remote Sensing and Spatial Information Sciences*.
- Seifert, E., Seifert, S., Vogt, H., Drew, D., van Aardt, J., Kunneke, A., & Seifert, T. (2019).

- Influence of Drone Altitude, Image Overlap, and Optical Sensor Resolution on Multi-View Reconstruction of Forest Images. *Remote Sensing*, 11(10), 1252. <https://doi.org/10.3390/rs11101252>
- Terpstra, T., Miller, S., & Hashemian, A. (2017). An Evaluation of Two Methodologies for Lens Distortion Removal when EXIF Data is Unavailable. *SAE Technical Paper Series*. <https://doi.org/10.4271/2017-01-1422>
- UK Civil Aviation Authority. (n.d.). *Registering to fly drones and model aircraft* | UK CAA. Retrieved 2025, from <https://www.caa.co.uk/drones/getting-started-with-drones-and-model-aircraft/registering-to-fly-drones-and-model-aircraft/>
- Westin, S. H. (2010). *ISO 12233 Test Chart*. <https://www.graphics.cornell.edu/~westin/misc/res-chart.html>
- Westoby, M. J., Brasington, J., Glasser, N. F., Hambrey, M. J., & Reynolds, J. M. (2012). “Structure-from-Motion” photogrammetry: A low-cost, effective tool for geoscience applications. *Geomorphology*, 179, 300–314. <http://dx.doi.org/10.1016/j.geomorph.2012.08.021>